

Thermal and electrical conductivity of melt mixed polycarbonate hybrid composites co-filled with multi-walled carbon nanotubes and graphene nanoplatelets

Marcin Wegrzyn,¹ Amaya Ortega,¹ Adolfo Benedito,¹ Enrique Gimenez²

¹Instituto Tecnológico del Plástico (AIMPLAS), Calle Gustave Eiffel 4, 46980 Paterna, Spain

²Instituto de Tecnología de Materiales, Universidad Politécnica de Valencia, Camino de Vera, 46022 Valencia, Spain

Correspondence to: M. Wegrzyn (E-mail: marcinwegrzyn@hotmail.com)

ABSTRACT: In this work, we present thermoplastic nanocomposites of polycarbonate (PC) matrix with hybrid nanofillers system formed by a melt-mixing approach. Various concentrations of multi-walled carbon nanotubes (MWCNT) and graphene nanoplatelets (GnP) were mixed in to PC and the melt was homogenized. The nanocomposites were compression molded and characterized by different techniques. Torque dependence on the nanofiller composition increased with the presence of carbon nanotubes. The synergy of carbon nanotubes and GnP showed exponential increase of thermal conductivity, which was compared to logarithmic increase for nanocomposite with no MWCNT. Decrease of Shore A hardness at elevated loads present for all investigated nanocomposites was correlated with the expected low homogeneity caused by a low shear during melt-mixing. Mathematical model was used to calculate elastic modulus from Shore A tests results. Vicat softening temperature (VST) showed opposite pattern for hybrid nanocomposites and for PC-MWCNT increasing in the latter case. Electrical conductivity boost was explained by the collective effect of high nanofiller loads and synergy of MWCNT and GnP. © 2015 Wiley Periodicals, Inc. *J. Appl. Polym. Sci.* **2015**, *132*, 42536.

KEYWORDS: composites; graphene and fullerenes; mechanical properties; nanotubes; thermal properties

Received 27 January 2015; accepted 25 May 2015

DOI: 10.1002/app.42536

INTRODUCTION

Thermoplastic polymer composites filled with carbon-based nanomaterials offer many solutions for material science.¹ Significant improvement of electrical and thermal properties of insulating polymers in these nanocomposites is attributed to the carbon nanotubes or graphene nanoplatelets (GnP) used as filler.^{2,3} A unique structure of these nanofillers provides also good mechanical performance of nanocomposites.^{4,5} These two aforementioned nanomaterials, often used separately as fillers,^{6,7} recently gained more attention as components of a hybrid systems-based nanocomposites.^{8,9} Complex engineering materials formed by co-filling thermoplastics with one- and two-dimensional fillers provide a broad range of opportunities for science and technology. However, a good quality interconnected network of nanofillers is necessary to reach the desired improvement of properties. The main problem distracting the performance of MWCNT and GnP is inefficient energy applied during processing disabling the breakage of nanofiller macrostructures causing inhomogeneous morphology of the final nanocomposite.¹⁰ This is related to the breakage of primary carbon nanotube agglomerates in the process of macrostructure penetration by polymer melt¹¹ or graphite exfoliation in order to obtain

monolayer sheets of GnP.¹² In a common nanocomposite formation by melt-mixing, the energy input is usually controlled by the parameter: specific mechanical energy (SME).¹³ Nevertheless, SME is convenient mainly for a continuous process and can be replaced in parameters influence analysis by torque. This is a desired solution when an internal mixer is used instead of a twin-screw extruder or when high nanofiller loads are used disabling microscopic methods of morphology determination.¹⁴

Intrinsic thermal conductivity of polymer-based materials is a key feature for processing and for application.¹⁵ Exfoliated or expanded graphene is reported to give good results improving the thermal conductivity of thermoplastic materials. The performance depends on the aspect ratio of the individual particles¹⁶ and the dispersion quality in the matrix.¹⁷ The latter factor seems to be crucial and Potschke *et al.*¹⁸ report that de-agglomeration during the melt mixing process gives excellent nanofiller dispersion in a representative polycarbonate (PC) matrix. However, often the high volume fractions of nanofillers are necessary for the desired increase of thermal conductivity, which restricts some of the commonly used processing methods such as extrusion or injection molding.¹⁹ Therefore, hybrid nanocomposites are the optimal solution to decrease filling load with maintaining

comparable thermal properties.²⁰ Hybrid fillers additionally induce morphological changes in the matrix (e.g., chains alignment), which has a positive effect on the thermal conductivity.²¹ A reported synergistic effect of carbon nanotubes and graphene in epoxy matrix show greater increase of thermal conductivity and mechanical properties for co-filled nanocomposites than for nanocomposites individually filled with each of these nanofillers.²² Besides, Vicat hardness as a parameter defining polymer softening point is improved with carbon nanotubes content which is reported for commodity polymers like polypropylene (PP) obtained by a twin-screw extrusion.²³ However, the balance of properties occurs at low loads (1–3 wt %) which suggests the occurrence of percolation threshold. Opposite observations reported for non-carbon fillers show a decreasing Vicat softening point with an increase of volume fraction.²⁴ Shore A hardness showing the values measured at room temperature increases with carbon nanotubes²⁵ and with two-dimensional (2D) silicate²⁶ concentration increase. Nevertheless, the change observed was clearly higher for the hybrid system combining these nanofillers. A correlation between the elastic modulus in compression and Shore A hardness was reported with a mathematical simulation of experimental data giving an acceptable agreement with *ca.* 5% error.²⁷ Thus, the theory of Boussinesq for comparison of both data sets is adequate. Furthermore, no modification of Shore A method in order to correlate the data with elastic modulus²⁸ was necessary. The aforementioned reports confirm that the dependence of mechanical performance on the various one- and two-dimensional fillers in a hybrid system exists. This is reported especially for the low-to-moderate filler concentrations.

In this work, we present PC-MWCNT/GnP nanocomposites prepared by melt-mixing in an internal mixer. Various nanofiller content and mutual nanofillers ratio allow studying the influence of synergistic effect on thermal and electrical conductivity. The study of torque during the nanocomposites formation shows the influence of nanofillers composition. Thermal conductivity and thermal effusivity were determined on a compression molded specimens with a Modified Transient Plane Source (MTPS) approach. Hardness measured at room temperature (Shore A) and Vicat hardness were determined in order to observe the influence of carbon nanotubes and GnP in hybrid system. A simple mathematical model was used in order to calculate the elastic modulus in compression from Shore A test data. Electrical conductivity measured with a two-point contact method is given in order to correlate electrical and thermal performance of the nanocomposites.

EXPERIMENTAL

Materials

Commercial polycarbonate (PC) Lexan EXL 6013 (MVR 5g/10 min) was supplied by SABIC Innovative Plastics. Multi-walled carbon nanotubes (MWCNT) NC7000 with average diameter 9.5 nm and average length 1.5 μm were supplied by Nanocyl. Graphene nanoplatelets (GnP) xGnP-M5 with thickness 6–8 nm and average particle diameter 5 μm were supplied by XG Sciences.

Preparation of Nanocomposites

Nanocomposites with various nanofillers concentrations shown in Table I were prepared on a Brabender Plasti-Corder PL-2000

Table I. Samples Codification and Nanofillers Content in Prepared PC-MWCNT/GnP Hybrid Nanocomposites

Sample code	Content	
	MWCNT	GnP
0T/0G	0.0 wt %	0.0 wt %
0T/1G	0.0 wt %	1.0 wt %
0T/5G	0.0 wt %	5.0 wt %
0T/10G	0.0 wt %	10.0 wt %
0T/15G	0.0 wt %	15.0 wt %
1T/0G	1.0 wt %	0.0 wt %
1T/1G	1.0 wt %	1.0 wt %
1T/5G	1.0 wt %	5.0 wt %
1T/10G	1.0 wt %	10.0 wt %
1T/15G	1.0 wt %	15.0 wt %
5T/0G	5.0 wt %	0.0 wt %
5T/1G	5.0 wt %	1.0 wt %
5T/5G	5.0 wt %	5.0 wt %
5T/10G	5.0 wt %	10.0 wt %
5T/15G	5.0 wt %	15.0 wt %

internal mixer at screw speed 120 rpm and barrel temperature 280°C. Polycarbonate (PC) was introduced to the mixing chamber and blended for 1 min until the torque was constant. Carbon nanotubes (MWCNT) and graphene nanoplatelets (GnP) were added to melted polycarbonate (PC) after this time and such formed nanocomposite was mixed for 9 min. PC-MWCNT/GnP nanocomposites subtracted from the mixing cavity were compression molded at 280°C on a Collin 6300 hydraulic press into the rectangular specimens with dimensions 25×25×5 mm³. A 25 min compression process was composed of five-steps with applied pressures varied between 5 bar and 140 bar.

Characterization

The tests were carried out on the compression molded specimens. Thermal conductivity of the nanocomposites was measured on a TCi TH89 Modified Transient Plane Source (MTPS) thermal conductivity analyzer (C-Therm Technologies). A one-sided heat reflectance sensor shown in Figure 1(a) provides a controlled amount of heat changing the temperature of a sample surface inducing the voltage drop. Two measurements [Figure 1(b)] were carried out for each of the five rectangular specimens at ambient temperature ($26.1 \pm 0.5^\circ\text{C}$) with deionized water used as a contact medium. Individual test included data collection step of 0.8 s and sensor cooling step between the data acquisition of 60 s.

Hardness of the nanocomposites was measured on an A-type Shore durometer. In this method, a standardized indenter was pressed by 8.064 N force into the specimen for 15 s at ambient temperature. After this time the hardness was determined based on the depth of indentation. Mathematical model was introduced in order to calculate the Elastic modulus from the hardness data.

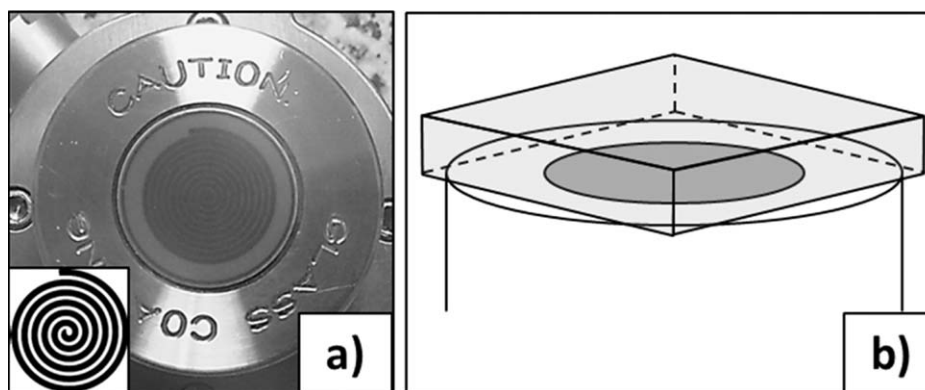


Figure 1. Methodology of thermal conductivity determination in hybrid PC-MWCNT/GnP nanocomposites: (a) top-view on the sensor with a pictogram showing the sensor outlay, (b) sample (gray) position on the sensor during measurement.

Vicat softening point was determined with B50 method following the EN ISO 306 standard. In this method, a flat-ended needle was constantly pressed by 50 N force into the specimen. Temperature of silicon oil used as a medium was raised from ambient with a rate $50^{\circ}\text{C h}^{-1}$.

Electrical resistivity was measured by a two-point contact configuration on a Keithley 2000 source meter. Silver electrodes were painted on the samples in order to improve contact between the specimen and the measuring electrodes.

RESULTS AND DISCUSSION

Each of the hybrid nanocomposites filled with carbon nanotubes (MWCNT) and graphene nanoplatelets (GnP) prepared with a single, 10 minutes-long processing step shows a decrease of torque with the homogenization of the melt (Figure 2 and Table II). The curves in Figure 2 represent torque during the formation of selected PC-GnP nanocomposites without carbon nanotubes. A clear increase of torque representing melt resistance to deformation during mixing increases with the nanofiller load until 10.0 wt % GnP. A change of nanocomposite behavior for material 0T/15G is explained by the lubricating properties of graphite, stronger at elevated loads. A 10.0 wt % GnP seems

to be the limit above which the agglomerates are large enough to disable strong nano-scale interactions between graphene and polymer chains. Above this concentration, the competition between the effect of lubricating properties of graphene and the effect of the formation of nanomaterial network that increases nanocomposite viscosity starts favoring the former one. Besides, intensification of the lubricating properties of graphene²⁹ at elevated loads facilitates the laminar flow of polymer melt in discrete layers.³⁰ Furthermore, the torque seems to be more constant above the eighth minute of processing (seventh minute of the nanocomposite mixing) for each investigated GnP concentration present in Figure 2. This reduction of the curve slope indicates the point of a relatively homogeneous nanocomposite. No significant improvement is expected with the increase of mixing time at the applied conditions, as from this moment the degradation of polymer matrix causing polymer chains shortening competes with the improvement of the nanofiller dispersion. On the contrary, the torque observed for PC decreases consecutively with the processing time and no plateau occurs, suggesting the influence of a slight polymer degradation caused by the temperature and the shear.

Further increase of torque is observed when carbon nanotubes are introduced to the system together with graphene (Table II).

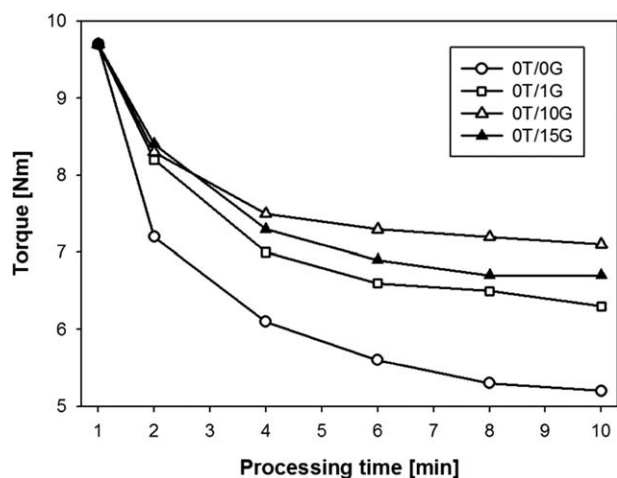


Figure 2. Torque during formation of PC-GnP nanocomposites at various processing stages.

Table II. Torque During Formation of Hybrid PC Nanocomposites Filled with Various Quantities of GnP and MWCNT

Sample	Torque			
	4 min	6 min	8 min	10 min
1T/0G	6.5 Nm	6.3 Nm	6.0 Nm	6.0 Nm
1T/1G	7.5 Nm	7.3 Nm	7.0 Nm	6.8 Nm
1T/5G	8.6 Nm	7.8 Nm	7.5 Nm	7.4 Nm
1T/10G	9.8 Nm	8.8 Nm	7.8 Nm	7.5 Nm
1T/15G	9.5 Nm	8.5 Nm	7.7 Nm	7.4 Nm
5T/0G	9.9 Nm	8.4 Nm	8.2 Nm	7.8 Nm
5T/1G	10.9 Nm	9.5 Nm	8.6 Nm	7.9 Nm
5T/5G	11.1 Nm	9.7 Nm	8.7 Nm	8.0 Nm
5T/10G	11.2 Nm	9.9 Nm	8.7 Nm	8.2 Nm
5T/15G	11.4 Nm	10.1 Nm	9.1 Nm	8.6 Nm

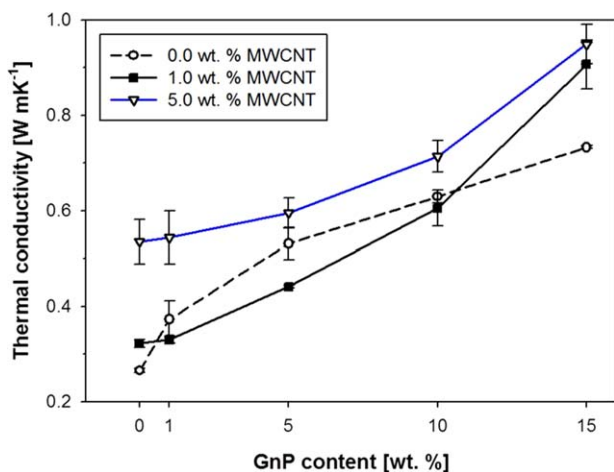


Figure 3. Thermal conductivity of PC-MWCNT/GnP hybrid nanocomposites. [Color figure can be viewed in the online issue, which is available at wileyonlinelibrary.com.]

During each individual process the torque shows a slightly different behavior to PC-GnP and an increase with the co-nanofiller (MWCNT) load is observed. Besides, the plateau observed for PC-GnP started at the eighth minute of processing does not occur when carbon nanotubes are introduced. Such an effect is most probably related to inhomogeneity of nanofillers dispersion after this processing time. Therefore, the processing time for hybrid nanocomposites formation in internal mixer should be balanced providing a good dispersion of nanofillers and the lowest possible matrix degradation. Data present in Table II shows a stronger increase of torque between 1T/1G and 1T/0G than for the further increase of GnP content. A *ca.* 13% torque increase is observed when 1.0 wt % GnP is introduced to the PC-GnP (forming a 1T/1G) and 8% increase for both, the 5.0 wt % GnP (1T/5G) and the 10.0 wt % GnP (1T/10G). This observation is confirmed also for the nanocomposites with 5.0 wt % MWCNT but the increase of torque is minor. Such an effect is related mainly to the type of nanofiller. Addition of GnP causes the formation of interconnected hybrid network increasing the viscosity of the nanocomposite. Besides, nanocomposites with the total nanofiller loads between 1.0 wt % and 2.0 wt % are most likely in the range of mechanical percolation, which should show the observed effect on torque. Similarly to the materials with no carbon nanotubes shown in Figure 2, the lower values of torque were observed at high nanofiller loads for nanocomposites 1T/15G than for 1T/10G. This is understood as a strong impact of the high total load of fillers, when the weight fraction is 15 wt % or 20 wt %. In this moment, the nano-scale interactions between the filler and the matrix are overcome by the lubricating properties of graphite and macro-scale carbon filler, since the significant part of MWCNT and GnP is not in the nano-scale anymore.

Besides, the nanocomposite 0T/1G (Figure 2) shows higher torque value than 1T/0G (Table II). The difference of *ca.* 6% observed above the sixth minute of processing indicates that graphene weakens the binding during the melt mixing processing due to its lubricating properties. Nevertheless, at low loads the penetration of carbon nanotube agglomerates by polymer

melt leading to the individually-dispersed nanoparticles seems to be easier than a good dispersion of GnP including the previous exfoliation. Reports show improved dispersion ability of nanomaterials in some hybrid systems.^{31,32} A relatively low shear rate during the nanocomposites preparation suggests non-efficient MWCNT agglomerates breakage and the formation of incomplete network in polymer matrix. Opposite effect with the synergy between carbon nanotubes and GnP is observed in nanocomposites with the total nanofiller load 6.0 wt %: 1T/5G and 5G/1T. Thus, the torque increases with an increase of MWCNT load and a decrease of GnP concentration. Material behavior changes at high nanofiller concentration so the efficiency of GnP dispersion in polymer matrix is reduced.³³

Thermal conductivity measured by the Modified Transient Plane Source (MTPS) approach (Figure 1) increases with the total nanofiller load for all investigated nanocomposites (Figure 3). The expected higher values for the hybrid compositions containing 5.0 wt % MWCNT were observed along the whole series. The curves recorded for the hybrid nanocomposites follow an exponential function ($657.9e^{0.041x}$ with $R^2=0.99$ for 1.0 wt % MWCNT and $893.0e^{0.022x}$ with $R^2=0.95$ for 5.0 wt % MWCNT) while the curve obtained for the PC-GnP is logarithmic ($89.9 \ln(x)+777.9$ with $R^2=0.92$). Similar effect is described in the literature as related with the quality of nanofiller dispersion.³⁴ Carbon nanotubes-based nanocomposites exhibit a logarithmic increase with the weight fraction when the material is homogeneous. On the other hand, poor dispersion of nanomaterials gives an exponential increase of thermal conductivity. The latter situation is most probably present in the nanocomposites with hybrid filler system present in this work. Low shear applied to the material was most probably insufficient to disperse the complex filler system properly. For the hybrid nanocomposites with 1.0 wt % MWCNT thermal conductivity is generally lower than for the PC filled only with GnP. This is attributed to the aforementioned synergy causing the decrease of torque for 1T/5G comparing to 5T/1G (Table II), having origins in the dispersion ability of one nanomaterial with the presence of another. Besides, the alignment of nanofiller is reported to play a key role in thermal conductivity performance of nanocomposites.³⁵ Such behavior is expected to change at high loads and for the material 1T/15G thermal conductivity is higher than for the 0T/15G. The effect of the increase of thermal conductivity at such high GnP load with the presence of 1.0 wt % MWCNT is probably related to the amount rather than the type of nanofiller.

A parameter K_{nc}/K_{mx} often used to represent the efficiency of material treatment on thermal properties is a ratio between the obtained thermal conductivity (K_{nc}) and thermal conductivity of a neat matrix (K_{mx}), a 0.261 WmK^{-1} for PC. Value generally increases with the increase of MWCNT and GnP load. Thus, regarding the highest studied GnP load of 15.0 wt %, the K_{nc}/K_{mx} gives values between 2.79 (0T/15G) and 3.33 (5T/15G). For significantly lower GnP concentration 1.0 wt %, K_{nc}/K_{mx} is between 1.23 (0T/1G) and 1.83 (5T/1G). This behavior is confronted with the PC-MWCNT nanocomposite without GnP and no significant change is observed for 1.0 wt % MWCNT before and after the addition of GnP (1T/0G and 1T/1G, respectively). This confirms the importance of the hybrid nanofiller system at

Table III. Thermal Effusivity of PC-MWCNT/GnP Nanocomposites Measured at 26.1 °C (± 0.5)

Sample code	Effusivity [$W s^{1/2} m^{-2} K^{-1}$]
0T/0G	610.57 (± 5.77)
0T/1G	729.26 (± 42.01)
0T/5G	860.00 (± 36.02)
0T/10G	990.22 (± 13.57)
0T/15G	1087.50 (± 2.93)
1T/0G	673.87 (± 9.73)
1T/1G	682.82 (± 8.93)
1T/5G	801.67 (± 33.17)
1T/10G	966.96 (± 37.64)
1T/15G	1252.13 (± 50.46)
5T/0G	906.79 (± 78.26)
5T/1G	935.56 (± 56.77)
5T/5G	957.57 (± 31.22)
5T/10G	1069.70 (± 31.46)
5T/15G	1275.19 (± 35.36)

high concentrations in order to boost the thermal conductivity of insulating polymer matrix.

Thermal effusivity of nanocomposites, e_{nc} , defined by eq. (1) is present in Table III. The values agree with the previous observations of thermal conductivity performance. The ability of the nanocomposite to absorb/exchange heat depends on the thermal conductivity of this nanocomposite, K_{nc} , its density, ρ_{nc} , and the specific heat capacity, c_p . A nearly linear increase of the thermal effusivity with an increase of GnP content is observed for the nanocomposites with no carbon nanotubes. Introduction of MWCNT and the formation of hybrid nanocomposites results with the exponential increase of effusivity with the increase of GnP load. Such a non-linear dependence is related to the presence of MWCNT-GnP interconnected network where a synergy of the hybrid nanofiller system increases the possible number of contacts between the particles. From a defined concentration the thermal performance changes significantly with a slight increase of the load. At 15.0 wt % GnP (1T/15G and 5T/15G) the thermal effusivity is almost equal for both nanocomposites, showing only 16.3% difference. This agrees with the aforementioned statement regarding upper level of the efficient nanofiller load.

$$e_{nc} = (K \rho_{nc} c_p)^{1/2} \quad (1)$$

Hardness of the nanocomposites measured by a Shore type A method is shown in Figure 4. An initial improvement of hardness is observed with the introduction of 1.0 wt % GnP, for materials 0T/1G and 1T/1G. The value between these nanocomposites does not differ significantly due to the effect of low nanofiller load.³⁶ Further development of the nanocomposites show that hardness decreases significantly, below the value recorded for the neat PC. Further increase of the total nanofiller load for both series shown in Figure 4 indicated the relative similarity between the material with 0.0 wt % MWCNT and the material with 5.0 wt % MWCNT occurs at low (1.0 wt %) and high (15.0 wt %) GnP

concentrations. Nevertheless, the values are clearly lower for PC-GnP than for the hybrid nanocomposite with 1.0 wt % MWCNT which confirms the aforementioned synergy. Besides, literature reports show the optimal size of grains in polymer matrix $d_c = 10$ nm providing the highest hardness.³⁷ The decrease of hardness below and above that defined grain size is correlated with the inter-granular processes. This theory can be adapted to the nanocomposites where a well-dispersed nanofiller phase meets the d_c requirement.³⁸ Furthermore, a filler-dependent nanocomposite hardness behavior was observed for PC-glass fiber/carbon nanotubes hybrid materials.³⁹ This is analogous to the behavior reported here. Thus, it seems that the concentration of macrostructures (micro-scale agglomerates) in the studied PC nanocomposites at GnP loads above 5.0 wt % is relatively high. Therefore, the explanation of the decrease of Shore A hardness can be related to the inhomogeneity of the material at elevated nanofiller loads.⁴⁰ However, at such high concentrations of carbon nanomaterials the transparency of the nanocomposite disables any statistically-supported analyses of micrographs revealing the quality of the morphology.

Modulus of elasticity in compression present in Table IV is determined basing on a Shore A hardness results.²⁷ Equation (2) defining the relationship between these parameters (E and Sh_A , respectively) includes the normalized radius of the indenter $R = 0.395$ mm, Poisson's ratio $\mu = 0.5$, and constants related to the relation between the depth of penetration and the Shore A hardness: $C_1 = 0.549$ N, $C_2 = 0.07516$ N, and $C_3 = 0.025$ mm. A standard deviation between the mathematical model and the experimental data is 5.4%.²⁷ Results of calculation show an increase (ca. 2.5%) of PC elastic modulus in compression after the formation of 0T/1G and 1T/1G. This initial increase of elastic modulus, analogous to the Shore A hardness, is followed by a significant decrease at elevated total nanofiller loads. A clear reduction of E is calculated with relatively high accuracy and can be related to the size of filler agglomerates. At elevated loads both nanofillers tend to exist in nanocomposites in the form of macrostructures, which causes a decrease of mechanical properties of the final material.

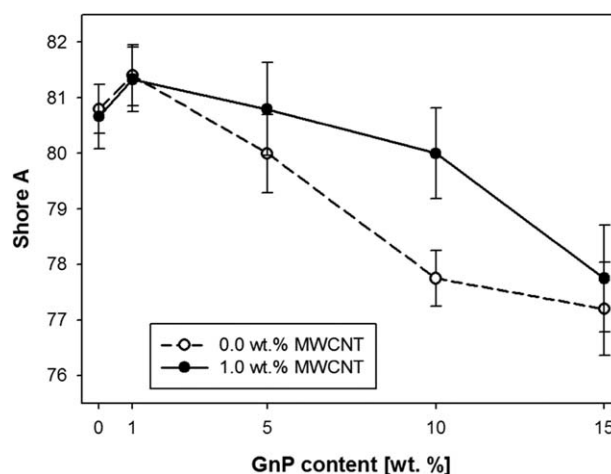
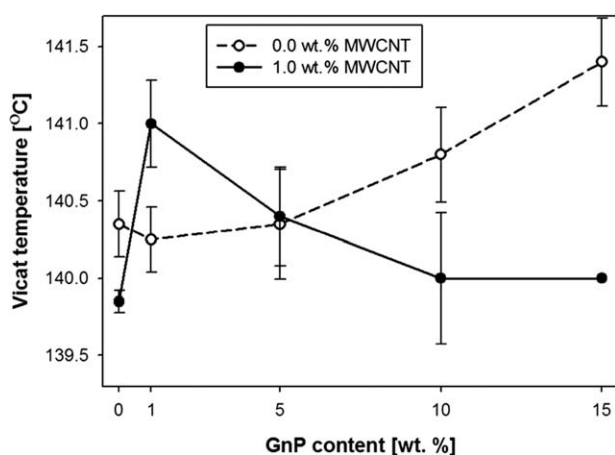
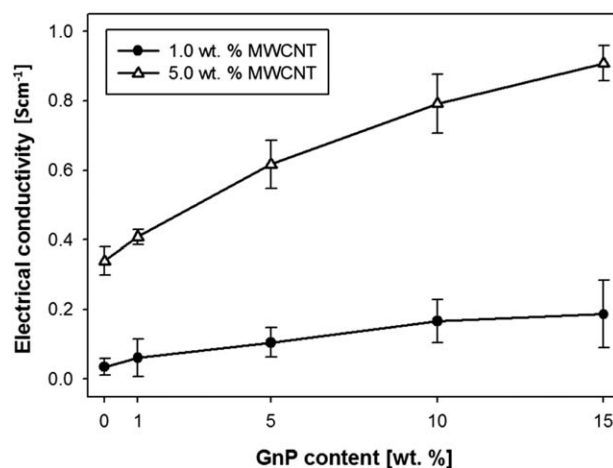
**Figure 4.** Shore A hardness of selected PC-MWCNT/GnP hybrid nanocomposites.

Table IV. Modulus of Elasticity in Compression Determined from Shore A Hardness

Sample code	Modulus of Elasticity [MPa]
0T/0G	12.89 (\pm 0.70)
0T/1G	13.23 (\pm 0.71)
0T/5G	12.46 (\pm 0.67)
0T/10G	11.40 (\pm 0.62)
0T/15G	11.17 (\pm 0.60)
1T/0G	12.81 (\pm 0.69)
1T/1G	13.19 (\pm 0.71)
1T/5G	12.89 (\pm 0.70)
1T/10G	12.46 (\pm 0.67)
1T/15G	11.40 (\pm 0.62)

$$E = \frac{1 - \mu^2}{2 \cdot R \cdot C_3} \cdot \frac{C_1 + C_2 \cdot Sh_A}{100 - Sh_A} \cdot (2.6 - 0.02 \cdot Sh_A) \quad (2)$$

Figure 5 with results of Vicat softening temperature (VST) of the selected nanocomposites shows a parameter behavior strongly dependent on the presence of carbon nanotubes. Usually a VST increase with the nanofiller load is reported in the literature,²³ similar to the pattern of the nanocomposite with 0.0 wt % MWCNT. An optimal load below 3.0 wt % nanofiller is reported to show the best Vicat temperature improvement for various nanofillers, which is in agreement with the findings present here.²³ Independently on the shape of the nanofiller, polymers exhibit an increase of the softening temperature at elevated weight fractions for one-dimensional (1D) carbon nanotubes²³ and 2D nanoclay.⁴¹ Since the VST is an indication of a temperature at which the specific value of Young's Modulus is reached, these results can be understood as an improvement of PC mechanical properties with the increase of GnP concentration. Nevertheless, some reports show, that the VST decreases when macro fibers⁴² or plasticizer⁴³ are added to the thermo-plastic matrix. These effects are related with the matrix degradation or with the decrease of Young's Modulus of the nanocomposite. Thus, the results shown of the hybrid nano-

**Figure 5.** Vicat softening temperature of selected PC-MWCNT/GnP hybrid nanocomposites.**Figure 6.** Electrical conductivity of selected PC-MWCNT/GnP hybrid nanocomposites.

composite with 1.0 wt % MWCNT shown in Figure 5 are related with analogous effects. Further increase of GnP concentration with the presence of 1.0 wt % carbon nanotubes causes the decrease of softening temperature. This most likely comes from the mutual interactions between the nanofillers of different geometries limiting the homogeneous dispersion of any component of the applied filler system. Initially, at low concentration of GnP and MWCNT an increase of the Vicat softening temperature (VST) is observed, confirming the capabilities of the applied system. Higher mixing energies and higher shear would most probably enable better dispersion of nanomaterials in PC, which would effect in the increase of VST.

Electrical conductivity values of the hybrid PC-based nanocomposites measured by a two-point method described elsewhere⁴⁴ are shown in in Figure 6 and in Table V. The improvement of electrical properties of PC/GnP in Table V shows the performance of four orders of magnitude increase of the virgin PC value for 1.0 wt % GnP (0T/1G). Besides, a significant improvement of electrical conductivity with the increase of GnP concentration occurs for both studied carbon nanotube loads (Figure 6). A 33.2% increase between 1T/0G and 1T/15G or a 167.0% increase between 5T/0G and 5T/15G shows the possible performance of the studied hybrid nanofiller system. Furthermore, a difference between the nanofillers is clear when the electrical conductivity performance for the same concentration is compared. The 0T/1G shows an increase of a *ca.* 10^{-4} Scm⁻¹ of the

Table V. Electrical Conductivity of Selected PC-MWCNT/GnP Nanocomposites

Sample code	Electrical conductivity [Scm ⁻¹]
0T/0G	1.00 E-14 (\pm 4.84 E-14)
0T/1G	1.04 E-10 (\pm 2.38 E-10)
0T/5G	7.59 E-08 (\pm 1.79 E-06)
0T/10G	2.53 E-05 (\pm 2.85 E-05)
0T/15G	5.60 E-04 (\pm 8.84 E-04)

PC value, while the 1T/0G gives 10^{-13} Scm $^{-1}$. Nevertheless, the effect of a hybrid filler system does not show significant difference favoring one nanofiller or another. Nanocomposite 1T/5G shows $1.0E-01$ Scm $^{-1}$ while 5T/1G, $4.1E-01$ Scm $^{-1}$, so both values show the improvement of electrical conductivity in the same order of magnitude. Such a boost observed for PC-MWCNT/GnP is attributed to a collective effect of high total nanofillers load and to the formation of interconnected hybrid network including two different types of nanofiller: one-dimensional (1D) nanotubes and two-dimensional (2D) GnP flakes. Possible junctions in the carbon nanotube-based conductive network are theoretically improved in this material, because the common contact scenarios (wall-to-wall, tip-to-wall, and tip-to-tip) include now more charge transfer options through the hybrid junctions MWCNT-GnP. Furthermore, a rather low shear during the whole processing does not affect the length of carbon nanotubes significantly, which is beneficial for the formation of the interconnected nanofillers network. Shortening of carbon nanotubes is reported to distract significant improvement of carbon nanotubes-based nanocomposites.⁴⁰

CONCLUSIONS

PC-based nanocomposites with a hybrid nanofillers system including multi-walled carbon nanotubes (MWCNT) and graphene nanoplatelets (GnP) show improvement of thermal and electrical conductivity of the virgin matrix. The nanocomposites with moderate-to-high loads of GnP provide significantly lower torque during melt mixing than the nanocomposites containing GnP and MWCNT. Such effect was attributed to the synergy between nanoparticles resulting in the formation of interconnected hybrid network in polymer melt, which increases viscosity and hampers screws rotation. Exponential boost of the thermal conductivity was explained with similar effect giving a 0.869 WmK $^{-1}$ for hybrid PC nanocomposite with 15.0 wt % GnP and 5.0 wt % MWCNT and 0.728 WmK $^{-1}$ with the absence of carbon nanotubes, an increase of the PC value of 233% and 180%, respectively. Hardness obtained in a Shore A test, used also to determine elastic modulus in compression, decreased at elevated nanofiller concentrations after an increase of the matrix value was recorded below the total nanofiller load of 5.0 wt %. A reduction of the VST for hybrid nanocomposites and the increase for PC-MWCNT is related with the insufficient shear provided during the formation of nanocomposite causing limited ability of agglomerates breakage and graphene exfoliation. A correct mutual concentration of nanofillers should be selected in order to achieve highest values of the studied parameters and this value should be kept on a rather low level, *c.a.* 3.0 wt % MWCNT+GnP. Electrical conductivity boost was observed to be dependent on the presence of carbon nanotubes and showed the collective effect of high nanofiller loads and synergy between carbon nanotubes and GnP. Thus, a further study that would include a more precise investigation of low weight volume fractions of both co-fillers and higher Specific Mechanical Energy (SME)⁴⁵ applied to the nanocomposite during the formation process is required.

ACKNOWLEDGMENTS

This work is funded by the European Community's Seventh Framework Program (FP7-PEOPLE-ITN-2008) within the CONTACT project Marie Curie Fellowship under grant number 238363.

REFERENCES

1. Su, I.; Schlögl, R. *Chem. Sus. Chem.* **2010**, *3*, 136.
2. Yang, L.; Liu, F.; Xia, H.; Qian, X.; Shen, K.; Zhang, J. *Carbon* **2011**, *49*, 3274.
3. Singh, I. V.; Tanaka, M.; Endo, M. *Int. J. Therm. Sci.* **2007**, *46*, 842.
4. Kuan, H. C.; Ma, C. C. M.; Chang, W. P.; Yuen, S. M.; Wu, H. H.; Lee, T. M. *Compos. Sci. Technol.* **2005**, *65*, 1703.
5. Arasteh, R.; Omid, M.; Rousta, A. H. A.; Kazerooni, H. J. *Macromol. Sci. B* **2011**, *50*, 2464.
6. Wegrzyn, M.; Benedito, A.; Gimenez, E. *J. Appl. Polym. Sci.* **2014**, *131*, 40271.
7. Cai, D.; Jin, J.; Yusoh, K.; Rafiq, R.; Song, M. *Compos. Sci. Technol.* **2012**, *72*, 702.
8. Martin-Gallego, M.; Verdejo, R.; Khayet, M.; Ortiz de Zarate, J. M.; Essalhi, M.; Lopez-Manchado, M. A. *Nanoscale Res. Lett.* **2011**, *610*, 1.
9. Yu, D.; Dai, L. *J. Phys. Chem. Lett.* **2010**, *1*, 467.
10. Haslam, M. D.; Raeymaekers, B. *Compos. B* **2013**, *55*, 16.
11. Pötschke, P.; Dudkin, S. M.; Alig, I. *Polymer* **2003**, *44*, 5023.
12. Stankovich, S.; Dikin, D. A.; Dommett, G. H.; Kohlhaas, K. M.; Zimney, E. J.; Stach, E. A.; Piner, R. D.; Nguyen, S. T.; Ruoff, R. S. *Nature* **2006**, *442*, 282.
13. Sathyanarayana, S.; Olowojoba, G.; Weiss, P.; Calgar, B.; Pataki, B.; Mikonsaari, I.; Huebner, C.; Hening, F. *Macromol. Mater. Eng.* **2013**, *298*, 89.
14. Ye, L.; Wu, Q.; Qu, B. *Polym. Degrad. Stabil.* **2009**, *94*, 751.
15. Ebadi-Dehaghani, H.; Nazempour, M. In *Smart Nanoparticles Technology – Thermal Conductivity of Nanoparticles Filled Polymers*; Hashim, A., Eds.; InTech: Shanghai, **2012**, p 519.
16. Kalaitzidou, K.; Fukushima, H.; Drzal, L. *Carbon* **2007**, *45*, 1446.
17. Mu, Q.; Feng, S.; Diao, G. *Polym. Compos.* **2007**, *28*, 125.
18. Pötschke, P.; Bhattachayya, A. R.; Janke, A. *Eur. Polym. J.* **2004**, *40*, 137.
19. King, J. A.; Barton, R. L.; Hauser, R. A.; Keith, J. M. *Polym. Compos.* **2008**, *29*, 421.
20. Hwang, Y.; Kim, M.; Kim, J. *Compos. A* **2013**, *55*, 195.
21. Babaei, H.; Keblinski, P.; Khodadadi, J. M. *Inter. J. Heat Mass Transfer* **2013**, *58*, 209.
22. Yang, S. Y.; Lin, W. N.; Huang, Y. L.; Tien, H. W.; Wang, J. Y.; Ma, C. C. M.; Li, S. M.; Wang, Y. S. *Carbon* **2011**, *49*, 793.
23. Pascual, J.; Peris, F.; Boronat, T.; Fenollar, O.; Balart, R. *Polym. Eng. Sci.* **2011**, *52*, 733.

24. Yasin, T.; Nisar, M.; Shafiq, M.; Nho, Y. C.; Ahmad, R. C. *Polym. Compos.* **2013**, *34*, 408.
25. Zhang, W. D.; Shen, L.; Phang, I. Y.; Liu, T. *Macromolecules* **2004**, *37*, 256.
26. Zhang, C.; Tjiu, W. W.; Liu, T.; Lui, W. Y.; Phang, I. Y.; Zhang, W. D. *J. Psych. Chem. B* **2011**, *115*, 3392.
27. Kunz, J.; Studer, M. *Kunstst. Int.* **2006**, *6*, 92.
28. Sponagel, S.; Unger, J.; Spies, K. H. *Kaut. Gummi Kunstst.* **2003**, *56*, 608.
29. Lin, J.; Wang, L.; Chen, G. *Tribol. Lett.* **2011**, *41*, 209.
30. Wagner, J. R.; Mount, E. M.; Giles, H. F. In *The Definitive Processing Guide and Handbook. Extrusion – Polymer Selection for Coextrusion*; Giles, H. F.; Wagner, J. R.; Mount E. M., Eds.; Elsevier: Oxford, **2014**; p 477.
31. Qiu, L.; Yang, X.; Gou, X.; Yang, W.; Ma, Z. F.; Wallace, G. G.; Li, D. *Chem. Eur. J.* **2010**, *16*, 10653.
32. Tian, L.; Meziani, M. J.; Lu, F.; Kong, C. Y.; Cao, L.; Thorne, T. J.; Sun, Y. P. *Appl. Mater. Interfaces* **2010**, *2*, 3217.
33. Potts, J.; Dreyer, D. R.; Bielawski, C. W.; Ruoff, R. S. *Polymer* **2011**, *52*, 5.
34. Song, Y. S.; Youn, J. R. *Carbon* **2005**, *43*, 1378.
35. Huang, H.; Liu, C. H.; Wu, Y.; Fan, S. *Adv. Mater.* **2005**, *17*, 1652.
36. Shokrieh, M. M.; Hosseinkhani, M. R.; Naimi-Jamal, M. R.; Tourani, H. *Polym. Test.* **2013**, *32*, 45.
37. Musil, J. In *Nanostructured Hard Coatings – Physical and mechanical properties of hard nanocomposite films prepared by reactive magnetron sputtering*; Cavaleiro, A.; De Hosson, J. T. M., Eds.; Kluwer Academic/Plenum Publishers: New York, **2006**; p 407.
38. Schiøtz, J. Proceedings of the 22nd Risø International Symposium on Materials Science: Science of Metastable and Nanocrystalline Alloys – Structure, Properties and Modelling; Dinesen, A. R., Eds.; **2001**, p 127.
39. Hornbostel, B.; Pötschke, P.; Kotz, J.; Roth, S. *Physica E* **2008**, *40*, 2434.
40. Gupta, T. K.; Singh, B. P.; Mathur, R. B.; Dhakate, S. R. *Nanoscale* **2014**, *6*, 842.
41. Pan, M.; Shi, X.; Li, X.; Hu, H.; Zhang, L. *J. Appl. Polym. Sci.* **2004**, *94*, 277.
42. Miranda, L. F.; Pereira, N. C.; Faldini, S. B.; Masson, T. J.; de Andrade e Silva, L. G.; Silveira, L. H. *Proc. Int. Nucl. Atlantic Conf.* **2009**.
43. Montanye, J. R.; Jnaicki, S. L. *Proc. ANTEC Conf.* **1991**, 1946.
44. Wegrzyn, M.; Juan, S.; Benedito, A.; Gimenez, E. *J. Appl. Polym. Sci.* **2013**, *130*, 2152.
45. Godavarti, S.; Karwe, M. V. *J. Arg. Eng. Res.* **1997**, *67*, 277.